Magneto-optical properties in ultrathin InAs-GaAs quantum wells

P. D. Wang, N. N. Ledentsov,* and C. M. Sotomayor Torres
Department of Electronics and Electrical Engineering, University of Glasgow, Glasgow G12 8QQ, United Kingdom

I. N. Yassievich, A. Pakhomov, A. Yu. Egovov, P. S. Kop'ev, and V. M. Ustinov
A. F. Ioffe Physico-Technical Institute, 26 Politekhnicheskaya Street, St. Petersburg 194021, Russia
(Received 27 January 1994; revised manuscript received 12 April 1994)

We determined exciton binding energies in monolayer InAs-GaAs quantum wells by studying photoluminescence excitation spectra in a magnetic field up to 8 T. The effective-mass approximation was used to caluclate the energy levels and determine the excitonic effects associated with Landau-level transitions and the exciton binding energy, which was also determined by extrapolation of higher-lying Landau-level transition energies to zero field. Both procedures lead to heavy-hole-exciton binding energies of the order of 10 meV, i.e., an enhancement of nearly 300% over bulk GaAs. From the diamagnetic shift of the exciton ground state, an estimate of the light-hole-exciton binding energy is made. In-plane effective mass reversal between heavy-hole- and light-hole-exciton states of submonolayer InAs was also observed. Furthermore, electron (exciton)-phonon coupling was also observed by level anticrossing, involving longitudinal as well as local vibrational phonon modes in ultrathin InAs.

I. INTRODUCTION

InAs/GaAs heterostructures are the most strained *III-V* compounds that have been studied. The lattice mismatch between InAs and GaAs amounts to 6.8%. Such highly strained system are interesting from their unique electronic and optical properties as well as for potential application in optoelectronic devices.[1]

Highly strained InAs/GaAs also provides a system for molecular-beam epitaxy (MBE) growth study. One to three monolayers (3 to 9 Å) can usually be deposited two dimensionally on GaAs by conventional MBE, further InAs deposition results in the formation of three-dimensional clusters, where dislocation can be formed when the clusters are large enough. Much thicker InAs layers (3 to 30 monolayers) can also be deposited in a two-dimensional fashion on GaAs, depending on the growth temperature and sequences.[2] It has been demonstrated that the microscopic origin of the strain relief can also occur through the surface roughness. Defects such as islands and steps at the surface of the strained layer allow a local strain partial relaxation. As a result, the growth becomes inhomogeneous, since preferential sites are available for subsequent incorporation. Indium segregation effects also smooth the interface abruptness and change the growth mode. All these effects will affect the optical properties of the InAs/GaAs system. In this paper, we will discuss the optical transitions observed in the InAs monolayers, and determine the associated exciton binding energy, based on the effective-mass approximation.

II. EXPERIMENT

The structures were grown by elemental source MBE side by side on (100) and (311)A-oriented GaAs semi-insulating substrates. An EP-1201 MBE reactor was used. Growth rates were 0.8 μm/h for GaAs and 0.3 μm/h for InAs. After oxide desorption, a 0.3-μm-thick GaAs buffer layer was grown at 600 °C. This layer was followed by a 40-period 25-Å GaAs/25-Å $Al_{0.4}Ga_{0.6}As$ superlattice (SL) to trap impurities and to prevent nonequilibrium carrier spreading into the semi-insulating substrate. The SL was followed by a 2000-Å GaAs layer, then the substrate temperature was lowered to 450 °C and the arsenic beam equivalent pressure was increased to 10^{-5} torr. After this, a 100-Å-thick GaAs layer was deposited which was followed by the InAs layer or an InAs-GaAs superlattice. Then, a 20-Å GaAs layer was grown on the top and the substrate temperature was increased to 600 °C, the arsenic pressure was reduced to 3×10^{-6} torr, and a 2000-Å-thick GaAs layer and 25-Å GaAs/25-Å $Al_{0.4}Ga_{0.6}As$ SL were grown on to prevent surface recombination and to avoid surface-related electric fields. Low substrate temperature and high arsenic pressure were used to minimize the In segregation effects.[3]

For photoluminescence (PL), PL excitation (PLE), and magneto-PLE studies, Ar^+ and Ti-sapphire lasers were used. PL signal was recorded using standard equipment with a spectral resolution of 0.2 meV. Optical fibers were used in magneto-PLE measurements. The back side of the samples was chemically polished and they were placed in paper holders to avoid any possible source of external strain.

III. RESULTS AND DISCUSSIONS

Figure 1 shows the energy dependence of the PLE peaks as a function of InAs monolayers deposited on GaAs, including previous results obtained in the literature.[4–6] We plot here results obtained only by PLE or transmission techniques. Large Stokes shifts are common in these InAs monolayers, rendering the photolumines-

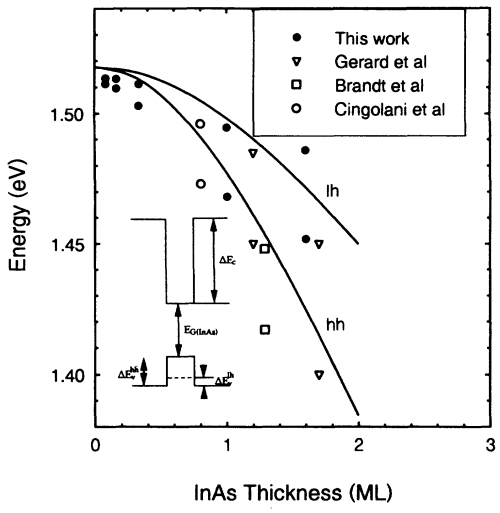

FIG. 1. The hh and lh energy transitions at 4 K versus InAs monolayer thickness grown by MBE. The hh and lh transitions were measured either by PLE or absorption measurement. 0.25 and 0.5-Å InAs were also included in addition to 1-Å, 1-ML, and 1.6-ML samples discussed in the text. The inset is the band alignment diagram for InAs/GaAs heterostructures. Solid lines in the figure are the effective-mass calculations based on the following strain-modified band parameters at 4 K: $E^0_{G(\mathrm{InAs})}=0.418$ eV, $E^0_{G(\mathrm{GaAs})}=1.518$ eV, $E_{G(\mathrm{InAs})}=0.533$ eV, $\Delta E_c=0.689$ eV, $\Delta E_v^{\mathrm{hh}}=0.295$ eV, and $\Delta E_v^{\mathrm{lh}}=0.089$ eV. The values are obtained assuming the InAs-GaAs system has a lattice mismatch of 6.8%.

cence results unreliable to determine the real transition energies. The solid line is an envelope function calculation without excitonic effects. The calculation takes into account the influence of strain and conduction band nonparabolicity. Both these effects have a large influence on the subband energies of InAs/GaAs. The conduction-band offset is assumed to be 70% of the band-gap difference.[5] For one monolayer (ML) sample, the heavy-hole (hh) valence-band potential $\Delta E_v^{\mathrm{hh}}=295.4$ meV, while light-hole (lh) valence-band offset $\Delta E_v^{\mathrm{lh}}=88.8$ meV. The lh is weakly bound in a type-I quantum-well structure. This is confirmed by the PLE spectrum where the relative intensity hh/lh is comparable to that found in GaAs-$Al_xGa_{1-x}As$ quantum wells for equivalent transitions, suggesting that lh states are localized in InAs monolayers. It can be seen that theory and experiments agree fairly well up to 2 ML. For thicker InAs layers, one should expect a much steeper energy decrease as a function of well thickness in the case of sharp interfaces. Effective-mass approximation and tight-binding models[7] predict similar results. Therefore, the strain relief mechanism is very important in the understanding of energy transitions beyond 1 ML. Another equally important mechanism is the segregation of indium during the MBE growth of GaAs on InAs. An InAs layer thickness smaller than 1 ML is treated here as a quasimonolayer. hh and lh exciton transitions were also confirmed by circular polarization PL and PLE measurements. The PL and PLE spectra for 0.3, 1, and 1.6 ML were presented in our previous paper.[3] Very high luminescence efficiency were observed in InAs monolayers.

When magnetic field is applied, a series of transitions associated with Landau levels evolves from the hh and lh exciton ground state transitions. Figure 2 shows the PLE spectra of a 1-ML InAs sample under various magnetic fields applied perpendicular to the InAs layers (parallel to the growth direction). All the transitions previously observed at zero magnetic field experience a diamagnetic shift, i.e., their energy is proportional to the square of the magnetic field. From the diamagnetic shift, the strength of the excitonic effects involved in the transitions can be determined. It should also be noted in Fig. 2 that energy level anticrossing at the first excited state can be observed at certain magnetic field.

Sharp lines related to GaAs-LO and InAs-LO phonons can also be observed in this sample. The nature of these sharp lines is attributed here to the resonant luminescence (RL), rather than the resonant Raman scattering, by measuring various polarization configurations, time dependence, as well as linewidth and temperature dependence. The details will be reported in a forthcoming pa-

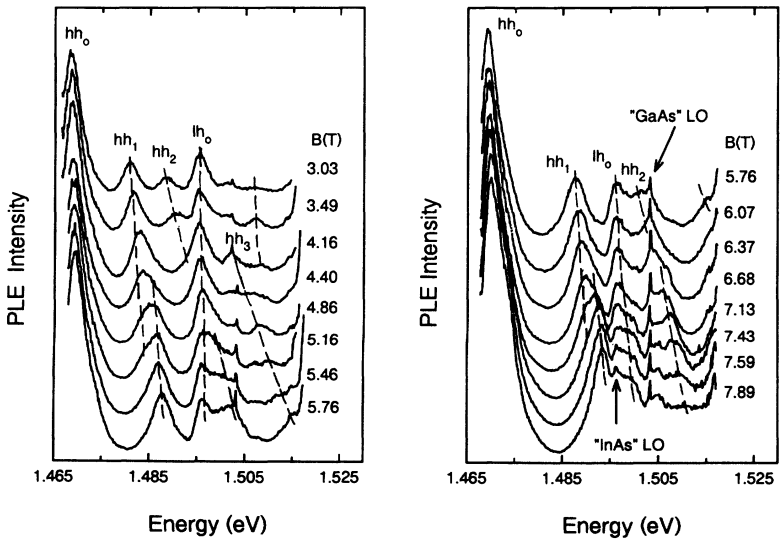

FIG. 2. Photoluminescence excitation spectra taken under different magnetic fields for a 1-ML InAs sample. The Landau-level anticrossing can be seen clearly for the first excited state of hh.

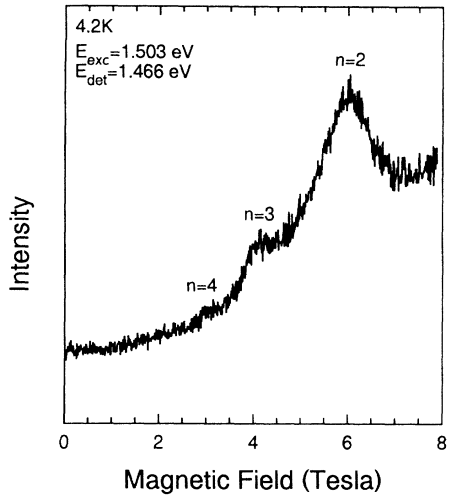

FIG. 3. Magneto-RL spectrum of 1-ML InAs. The excitation and detection energies are set at 1-LO-phonon energy difference. The transition efficiency undergoes a resonance when the excitation photon is resonant with various inter-Landau-level transitions involving excited excitonic states.

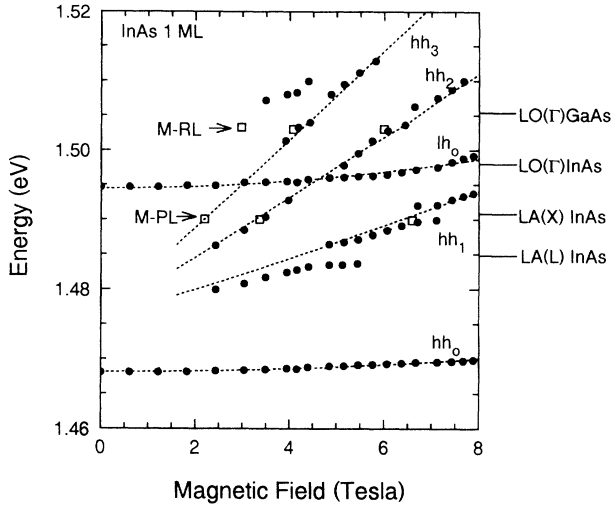

FIG. 4. Transition energies as a function of magnetic field for the 1-ML InAs sample. The dashed line is the theoretical fit (see text for details). The extrapolation method is not shown here and the value is discussed in the text. Landau-level crossover can be seen clearly with InAs LA phonons at the zero boundary. Magneto-RL data, labeled as *M*-RL, shown in Fig. 3 is also included in the plot. The other array of data labeled *M*-PL is the magnetophotoluminescence: it is the photoluminescence intensity profile versus magnetic field under resonant excitation conditions. Luminescence intensity shows resonance features when the excitation is resonant with inter-Landau-level transitions.

per. Nevertheless, it is usually unnecessary to distinguish the two processes, especially under resonant excitations. This observation enables us to perform magneto-RL spectrum in 1-ML InAs. In this spectrum (Fig. 3), the detector and excitation energy are set at one LO-phonon energy difference. The efficiency for the sharp lines exhibits resonant structure which can be associated with interband magneto-optical transitions between Landau levels. In 1- and 1.6-ML samples, the RL process is readily found to occur in doubly resonant conditions.[8] The dependence of the transition energies of the 1-ML sample upon magnetic field is shown in Fig. 4. The Landau-level transitions can be observed at fields as low as 2 T, indicating the high optical quality of the samples. The energies at which Landau levels shows anticrossing effects are found to match those of InAs LA phonons at the zone boundary (*X* and *L*), measured with respect to the hh ground state. Magnetopolaron effects at LO-phonon energy may also exist (see Fig. 3), but cannot be identified clearly due to the rather complicated spectrum in that regime. PLE experiments at higher magnetic fields (up to 20 T) are under way in order to clarify this issue. The resonances seen in magneto-RL data have also been indicated and agree very well in the fan chart plot. Other data determined by resonant magneto-PL has been indicated as well. Figure 5 shows a similar fan chart diagram for the 1.6-ML InAs sample. The Landau-level crossover due to interband magnetopolaron effects can also be seen clearly. As in the case of the 1-ML sample, the phonons involved are zone-boundary LA phonons of InAs. For both the 1 and 1.6-ML sample, the energy splitting of the transitions at the LA-phonon energies amounts to ~ 2 meV, indicating quite strong magnetopolaron coupling.[9] We show in Fig. 6 the transition dependence of the 1-Å sample (a third of a monolayer on average). Only one excited state of the hh exciton can be observed. Other transitions are above the continuum of bulk GaAs exciton states. Also plotted in Fig. 6 is the geminate recombination data at two different exciton energies. Such geminate (electron-hole pair) recombination with the energy close to exciting photon energy has been reported previously in GaAs quantum wells on application of a strong

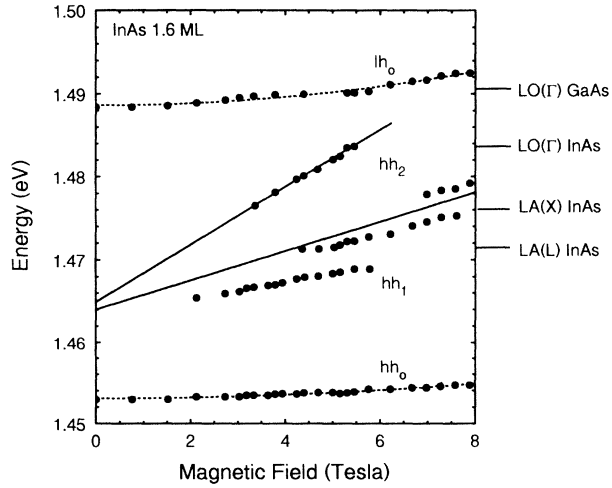

FIG. 5. Transition energies as a function of magnetic field for the 1.6-ML InAs sample. The remarkable feature is the Landau-level anticrossing effect, similar to the 1-ML InAs sample. The solid line is the extrapolation from high magnetic field to 0 T. The binding energy determined by this procedure is 12.0±0.5 meV.

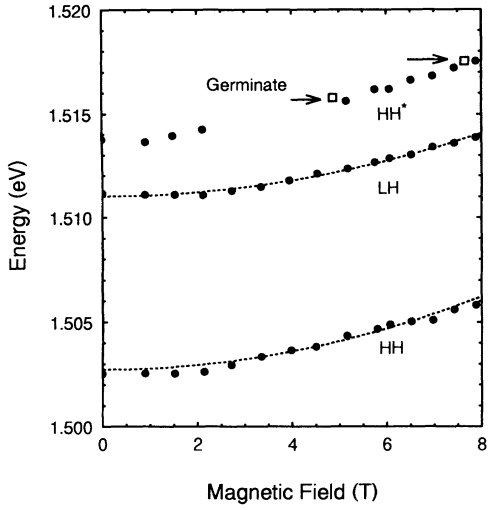

FIG. 6. The Landau-level fan-chart for the 0.3-ML (1 Å) InAs sample. The higher transitions are above the GaAs continuum, not readily resolved. Two-pair (geminate) recombination data under strong magnetic fields are also plotted for two different excitation energies.

magnetic-field perpendicular to the heterojunction planes.[10] Such observation in InAs submonolayers confirmed the Landau-level transitions in PLE spectra (see Fig. 6). Landau-level transitions in the bulk GaAs matrix can also be observed by monitoring the InAs luminescence. This is due to the very efficient carrier trapping from the excited GaAs volume to the InAs quantum well. We therefore can determine the GaAs exciton binding energy simultaneously.

(a) *Exciton binding energy.* The exciton binding energy can be measured by extrapolating the high Landau-level transition energies to zero field. The converging point at $B=0$ T is the onset of exciton continuum states. The energy difference between the converging point and the ground-state transition is the exciton binding energy.[11,12] Table I lists the exciton binding energy in different samples.

In these ultrathin InAs-GaAs quantum wells, using the envelope function approach, the InAs quantum-well wave function penetrates very deeply in the GaAs barrier. This is confirmed in the resonant Raman-like spectra where the main LO-phonon energy is 36.5 meV approaching the bulk GaAs phonon mode.[8] We assume here an effective mass, close to that of the GaAs barrier, for the whole InAs-GaAs system and perform the same effective-mass calculation. Such a calculation reveals the same energy transitions as those discussed earlier in Fig. 1. The effective mass for the 1-ML sample is chosen to be $m_e^*=0.061m_0$, $m_{\rm hh}^*=0.50m_0$. Hence the conduction-band dispersion under magnetic field is

$$E_e(B,n)=\frac{(2n+1)\hbar eB}{2m_e^*}+E_e^0 . \tag{1}$$

Similarly, the hh valence-band energy is given by

$$E_{\rm hh}(B,n)=\frac{(2n+1)\hbar eB}{2m_{\rm hh}^*}+E_{\rm hh}^0 . \tag{2}$$

We include the excitonic effects in calculating inter-Landau-level transitions.[13,14] This analysis is based on the work of Akimoto and Hasegawa,[14] in which the Zeeman-shifted states of hydrogenic excitons lead to the excitonic states bound between electron and hole Landau levels. In the limit of high magnetic field, the exciton binding energy is[13]

$$E_B\approx 3\left[\frac{\hbar eB}{2(2n+1)\mu_{\rm exc}^* R^*}\right]^{1/2} R^* D_1 , \tag{3}$$

where $\mu_{\rm exc}^*$ is the exciton reduced mass and R^* is the exciton effective Rydberg. D_1 is a parameter related to the dimensionality of the exciton, ranging from 0.25 in three dimension (3D) to 1.00 in two dimension (2D); the zero-field exciton binding energy is given by $E_B(0)=4R^*D_1$. The dashed line for hh excited states in Fig. 4 shows such a fit with only one adjustable parameter D_1. D_1 is found to be 0.63 ± 0.04 to give the best fit for the experimental data of 1-ML InAs. The binding energy determined by this theoretical fit is 9.9 meV, slightly larger than the extrapolation method, where the excitonic effects for higher lying Landau levels were not considered.

As stated above, ground-state exciton transitions shift quadratically with magnetic field. These excitons have the highest exciton Coulombic energy. The energy shift for the ground state is

$$\Delta E=D_2\frac{\hbar^2e^2B^2}{8\mu_{\rm exc}^{*\,2}R^*} . \tag{4}$$

D_2 is another dimensionality parameter, $D_2=1$ for a

TABLE I. Exciton binding energies (in meV) and diamagnetic shift in InAs monolayers on the GaAs matrix. See text for details. Δ denotes a value that is measured from the energy separation between ground and excited states of the hh exciton.

		GaAs	0.3 ML	1 ML	1.6 ML	2D
hh	Extrapolation	4.5±0.2	$>11.2^{\Delta}$	8.0±0.5	12.0±0.5	18.0
	$E_B(0)=4R^*D_1$	4.8±0.5		9.9±0.2	10.2±0.5	19.2
	E/B^2 (μeV/T^2)	77.1	54.5	28.8	27.8	14.6
	D_1	0.25		0.63	0.65	1
	D_2	1		0.36	0.30	0.188
lh	$E_B(0)=4R^*D_1$			5.07±0.2	5.16±0.2	
	E/B^2 (μeV/T^2)		47.8	65.9	63.9	

purely 3D and $\frac{3}{16}$ for a purely 2D exciton states. In ultrathin InAs/GaAs quantum wells, the dimensionality parameter D_1 and D_2 can be drastically different for different thickness of the sample, depending on the real interface structure, in-plane coalescence, and strain relaxation mechanism. Here we can only discuss qualitatively the excitonic effects from its diamagnetic shift. As can be seen in Table I, heavy-hole excitons of 1 and 1.6 ML samples have similar diamagnetic dependence. If one assumes they have the same dimensionality parameters, 1.6-ML hh exciton binding energy can be calculated to be 10.2 meV. The lh excitons exhibit a much larger diamagnetic shift, close to the bulk GaAs. This is, in fact, not surprising since the light hole is weakly confined under strong biaxial compression strain. One would expect that its exciton binding energy should also be weaker, comparable to that of GaAs bulk exciton. Phenomenologically, if one takes D_1 and D_2 to be the same as those in a 3D system, the lh exciton binding energies are 5.05 and 5.15 meV in the 1 and 1.6-ML samples, respectively. Such interpretation is consistent with the weak confinement of light holes modified by the strain.

Interestingly, the 0.3-ML sample exhibits the effective-mass reversal as shown by its diamagnetic shift (see Table I). Two mechanisms can be accounted for for the in-plane effective-mass reversal between hh and lh exciton states. Strong strain due to lattice mismatch induces in-plane coupling between hh and lh states.[15] The other mechanism arises from the observation of optical anisotropy in this submonolayer InAs sample. This is due to the preferential growth mechanism during the first stage of InAs deposition.[3] InAs molecules form the strings along $[1\bar{1}0]$ direction with monolayer width. It can be therefore viewed as quantum wire arrays. One-dimensional nature of the 0.3-ML InAs can enhance the effective-mass reversal and even exhibit electronlike states.[16] Both of these mechanisms are less pronounced in 1 and 1.6 ML, partly due to the weak confinement of lh. Here one should also notice that effective-mass theory may not be valid in this regime since InAs does not cover a whole layer. Optical and magneto-optical properties of submonolayer InAs are exhibiting very high luminescence efficiency, exciton effective-mass reversal, and large separation between ground and excited heavy-hole exciton states. This system is so unique that it will require further investigations.

The InAs monolayers embedded in the GaAs matrix can be viewed as a sheet of isoelectronic impurities in the bulk GaAs. In the theoretical description of these states, it has been suggested the electrically neutral isoelectronic substituent must first trap one-electronic particle, whereupon a second particle of opposite type can become bound in the Coulomb field of the first to form the bound exciton state.[17] The first particle is bound to the impurity atom by short-range non-Coulombic forces. Furthermore, the first particle to be trapped can be predicted from a consideration of the difference in the electronegativities of the impurity atom and the atom it replaces. Such isoelectronic impurities have been reported, e.g., in GaP doped with N or Bi atoms,[18] CdS,[19] and recently in ZnSe quantum wells doped with Te.[20] In GaAs doped with In, the hole wave function is expected to be trapped and compressed. Thus electrons can gain Coulomb interaction energy. This gain in interaction energy is eventually balanced by the increase in the kinetic energy of the hole. This explains very high exciton binding energy, even in the case of ultrahigh (monolayer) quantum wells.

Based on the above discussions, we propose a variational approach in the exciton binding-energy calculations. The binding energy of the ground state of heavy-hole excitons is determined mostly by electron motion when $m_e/m_{\rm hh} \ll 1$. In the case of very narrow quantum wells (QW), the effect of QW can be taken into account by introducing into the electron Hamiltonian the following pseudopotential:

$$V(z) = -\frac{\hbar^2}{m_e}\theta\delta(z) , \tag{5}$$

where $\theta = \sqrt{2m_eE}/\hbar$, E is the size quantization measured from the conduction band of bulk GaAs. δ is the function. This approximation is valid for deep and narrow QW's with the well width $L \ll a_B$ and band offset $V \gg E_B$. Here a_B and E_B are the Bohr radius and exciton binding energy. The trial function[21] is

$$\psi_\lambda = \exp\left\{-\frac{\lambda\rho}{a_B} - \theta|z|\right\} , \tag{6}$$

where λ is the variational parameter and $\rho = \sqrt{x^2+y^2+z^2}$. The variational solution of Schrödinger equation with the Coulomb potential and pseudopotential (5) leads to the exciton binding energy of

$$E_{\rm ex} = 2E_B\{\lambda_0(1+\sqrt{\lambda_0-1}) - \lambda_0^2/2\} , \tag{7}$$

where $\lambda_0(\theta a_B)$ is determined by minimizing the system expectation value. The dependence of $E_{\rm ex}$ on the well parameter θ is presented by the solid line in Fig. 7. The experimental data are from Table I for 0.3-, 1-, and 1.6-ML InAs studied in this paper. As discussed before in this section, the 0.3-ML InAs shows pronounced island formation and even wirelike arrays of monolayer width. Therefore, the 0.3-ML InAs should exhibit enhanced exciton localization and enhanced exciton binding due to its 1D nature. This may explain the larger discrepancy in

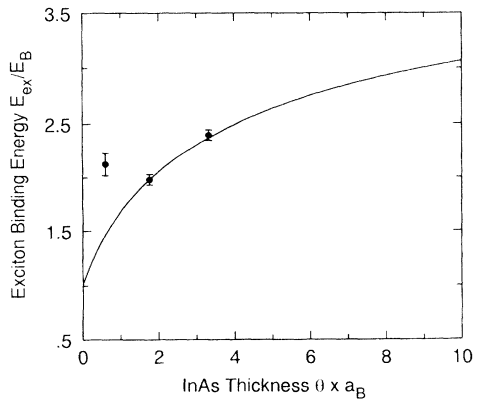

FIG. 7. Theoretical (solid line) and experimental (●) exciton binding energies in ultrathin InAs quantum wells.

Fig. 7 for the 0.3-ML InAs sample. With further reduction of average InAs thickness, the exciton binding energy should approach that of GaAs, as can be seen in Fig. 1 for 0.25 and 0.5-Å InAs.

(b) *Interband magnetopolaron effects.* For the 1-ML sample, as can be seen from the PLE spectra (Fig. 2) and fan-chart diagram (Fig. 4), Landau-level anticrossing was observed very clearly for the first excited state of hh exciton transitions (2*s* state). The energies at which level anticrossing effects occur are 17.6 and 20.0 meV, as measured with respect to the hh exciton ground state (1*s* state). We want to point out that although these energies appear to match those of strained InAs LA phonons at the zone boundary (*L* and *X*), local vibrational phonon mode involving In, Ga, and As atoms may take part in the process. This is typical for ultrathin InAs monolayers. Interface disorder can sufficiently breakdown the momentum conservation and plays a crucial role in recombination and scattering processes in the case of monolayer-thick quantum wells. The maximum energy splitting amounts to ~ 2 meV (see Fig. 4). Identical splitting and level crossing effects were observed in the 1.6-ML sample. This is shown in its fan-chart diagram of Fig. 5. Furthermore, the pinning effects at these two levels indicate strong resonant interactions involving phonon modes. For our awareness, this is the first report on interband resonant magnetopolaron effects involving exciton states.

In bulk materials, this anticrossing effect was first observed by Johnson and Larsen[22] who reported the anomalous interband magnetoabsorption experiments in InSb at 30 K with magnetic field up to 4 T. In the absence of electron-phonon coupling, the observed line would correspond to a transition between a heavy-hole $n=3$ spin-orbit valence-band level and $n=1$ spin-up conduction-band level. At $B>3.2$ T, a notable anticrossing was observed. This is due to the fact that Landau level $n=1$ is coupled to the state $n=0$ plus one phonon. The effect of coupling is to remove the degeneracy at the $\omega_c=\omega_{\mathrm{LO}}$ and causes the unperturbed levels to repel one another. Thus two branches were observed for this transition.

In quantum-well structures, much attention has been devoted recently to a single-particle system involving hydrogenic donors in GaAs QW's.[9] Strong magnetopolaron coupling has been observed and interpreted in terms of both Fröhlich interactions with bulk LO phonons[23] as well as confined and interface optical-phonon modes.[24] Theoretical calculations generally involve a variational approach in the unperturbed energy levels. Polaron corrections are introduced through second-order perturbation theory. The chosen trial functions are vitally important in order to account for the resonant polaron coupling. Enhanced magnetopolaron effects are observed partly due to the phonon confinement where multiphonon modes (including the macroscopic interface phonons in superlattices) are involved in the electron-phonon interactions.

Polaron effects in a bulk Wannier exciton have been investigated by Bajaj[25] who calculated the exciton ground-state energy with polaron corrections. Such work has been extended recently to quantum-well structures.[26,27] Polaron corrections on the exciton binding energy have been investigated as a function of QW thickness. However, resonant coupling has not been investigated theoretically so far.

The level anticrossing reported in this work suggested a coupling mechanism of the first excited hh (2*s*) state and hh (1*s*) ground state plus one phonon. The exact modeling should await for a further and thorough understanding of the phonon vibrational modes in the ultrathin InAs-GaAs system. The microscopic strain effects surrounding these monolayers should also be studied. It is worthwhile to point out that the band mixing induced anticrossing due to complicated valence-band structures in a wider quantum well should be excluded from our observations. Such effects have been investigated both theoretically by Bauer and Ando[28] based on an effective-mass approximation and experimentally by Viña *et al.* on *p-i-n* QW structures using magnetophotoluminescence excitation spectroscopy.[29] States belonging to the same irreducible representation can couple and exhibit anticrossing effects. In the magnetic field and transition regime relative to this work, hh (2*s*-) and lh (3*d*-) exciton states have the same symmetry (Γ_{7g}) and interact by repelling each other and sharing the oscillator strength. In the very narrow quantum wells studied here, the theoretical work by Bauer and Ando[28] is expected to be less accurate. Qualitively, lattice-mismatch induced strain field shifts the lh valence band considerably as illustrated in the inset of Fig. 1. Therefore, the crossing effect between lh (3*d*-) and hh (2*s*-) exciton states did not occur below 8 T. This is clear from the fan chart diagram of Figs. 4 and 5.

IV. CONCLUSION

We have performed the magneto-optical studies of ultrathin InAs/GaAs monolayers. The hh exciton binding energy can be determined to be ~ 12 meV for 1 and 1.6-ML samples, while lh exciton states are weakly bound due to the very large strain effects. The binding energy is enhanced by nearly 300% compared to that of bulk GaAs, and is considerably larger than those reported in Ref. 6 in a comparable sample arrangement. Strong heavy-hole exciton confinement is confirmed both by a strongly reduced diamagnetic shift and enhanced exciton binding energies. Submonolayer InAs exhibits the effective-mass reversal and can be accounted for by strain and 1D effects. Carrier-phonon interactions can also be observed as Landau-level anticrossing effects. This may originate from the strong influence of strain and monolayer fluctuations in InAs/GaAs heterostructures.

ACKNOWLEDGMENTS

The authors are grateful to A. Ross for technical support. Support from the NATO Linkage Grant No. 921378 and the UK SERC Grant No. GR/H4474 is gratefully acknowledged. N.N.L., V.M.U., and P.S.K. thank the International Science Foundation for individual financial support.

*On leave from A. F. Ioffe Physico-Technical Institute, 26, Politekhnicheskaya Street, St. Petersburg, 194021, Russia.

[1]E. P. O'Reilly, Semicond. Sci. Technol. **4**, 121 (1989).

[2]F. J. Grunthaner, M. Y. Yuen, R. Fernandez, T. C. Lee, A. Madhukar, and B. F. Lewis, Appl. Phys. Lett. **46**, 983 (1985).

[3]P. D. Wang, N. N. Ledentsov, C. M. Sotomayor-Torres, P. S. Kop'ev, and V. M. Ustinov, Appl. Phys. Lett. **64**, 1526 (1994).

[4]J. M. Gerard and J. Y. Marzin, Appl. Phys. Lett. **53**, 568 (1988).

[5]O. Brandt, L. Tapfer, R. Cingolani, and K. Ploog, Phys. Rev. B **41**, 12 599 (1990); see also, O. Brandt, R. Cingolani, H. Lage, G. Scamarcio, L. Tapfer, and K. Ploog, *ibid.* **42**, 11 396 (1990).

[6]R. Cingolani, O. Brandt, L. Tapfer, G. Scamarcio, G. C. La Rocca, and K. Ploog, Phys. Rev. B **42**, 3209 (1990).

[7]M. A. Tischler, N. G. Anderson, and S. M. Bedair, Appl. Phys. Lett. **49**, 1199 (1986).

[8]P. D. Wang, N. N. Ledentsov, C. M. Sotomayo-Torres, P. S. Kop'ev, and V. M. Ustinov (unpublished).

[9]J. P. Cheng, B. D. McCombe, J. M. Shi, F. M. Peeters, and J. T. Devreese, Phys. Rev. B **48**, 7910 (1993); also, J. P. Cheng, B. D. McCombe, G. Brozak, and W. Schaff, *ibid.* **48**, 17 243 (1993).

[10]P. S. Kop'ev, D. N. Mirlin, V. F. Sapega, and A. A. Sirenko, Pis'ma Zh. Eksp. Teor. Fiz. **51**, 624 (1990) [JETP Lett. **51**, 708 (1990)].

[11]J. C. Maan, G. Belle, A. Fasolino, M. Altarelli, and K. Ploog, Phys. Rev. B **30**, 2253 (1984).

[12]D. C. Rogers, J. Singleton, R. J. Nicholas, C. T. Foxon, and K. Woodbridge, Phys. Rev. B **34**, 4002 (1986).

[13]Q. H. F. Vrehen, J. Phys. Chem. Solids **29**, 129 (1968).

[14]O. Akimoto and H. Hasegawa, J. Phys. Soc. Jpn. **22**, 181 (1967).

[15]See, e.g., R. People and S. A. Jackson, in *Semiconductors and Semimetals,* edited by T. P. Pearsall (Academic, New York, 1990), Vol. 32 Chap. 4, p. 119.

[16]M. Sweeny, J. M. Xu, and M. Shur, Superlatt. Microstruct. **4**, 623 (1988).

[17]J. J. Hopfield, D. G. Thomas, and R. T. Lynch, Phys. Rev. Lett. **17**, 312 (1966).

[18]D. G. Thomas, J. J. Hopfield, and C. J. Frosch, Phys. Rev. Lett. **15**, 857 (1965).

[19]J. D. Cuthbert and D. G. Thomas, J. Appl. Phys. **39**, 1573 (1968).

[20]Q. Fu, D. Lee, A. V. Nurmikko, L. A. Kolodziejski, and R. L. Gunshor, Phys. Rev. B **39**, 3173 (1989).

[21]R. G. Green, K. K. Bajaj, and D. E. Phelps, Phys. B **29**, 1807 (1984).

[22]E. J. Johnson and D. M. Larsen, Phys. Rev. Lett. **16**, 655 (1966).

[23]M. Shi, F. M. Peeters, G. Q. Hai, and J. T. Devreese, Phys. Rev. B **44**, 5692 (1991).

[24]D. L. Lin, R. Chen, and T. F. George, Phys. Rev. B **43**, 9328 (1991).

[25]K. K. Bajaj, in *Polarons in Ionic Crystals and Polar Semiconductors,* edited by J. T. Devreese (North-Holland, Amsterdam, 1972), p. 193, and references therein.

[26]M. H. Degani and O. Hipolito, Phys. Rev. B **35**, 4507 (1987).

[27]M. Matsuura, Phys. Rev. B **37**, 6977 (1987).

[28]G. E. W. Bauer and T. Ando, Phys. Rev. B **38**, 6015 (1988).

[29]L. Viña, G. E. W. Bauer, M. Potemski, J. C. Maan, E. E. Mendez, and W. I. Wang, Surf. Sci. **229**, 504 (1990).